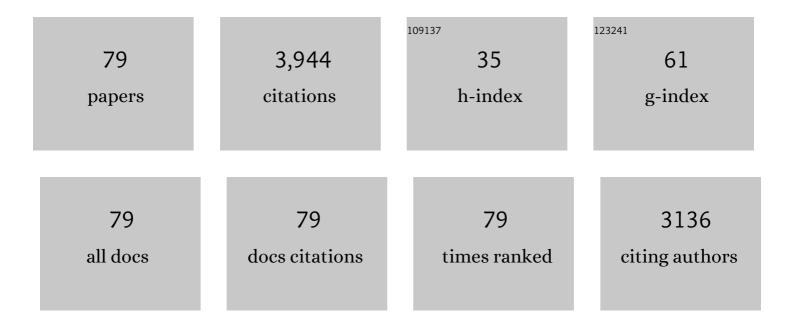
## List of Publications by Year in descending order

Source: https://exaly.com/author-pdf/7158213/publications.pdf Version: 2024-02-01



SONG HU

#	Article	IF	CITATIONS
1	Evolution of coke structures during electrochemical upgrading of bio-oil. Fuel Processing Technology, 2022, 225, 107036.	3.7	11
2	Coke formation during the pyrolysis of bio-oil: Further understanding on the evolution of radicals. Applications in Energy and Combustion Science, 2022, 9, 100050.	0.9	3
3	Evolution of char structure during the pyrolysis of biomass pellet: Further understanding on the effects of chars two phases. Fuel, 2022, 312, 122994.	3.4	10
4	A novel sludge pyrolysis and biomass gasification integrated method to enhance hydrogen-rich gas generation. Energy Conversion and Management, 2022, 254, 115205.	4.4	25
5	Pyrolysis reaction mechanism of typical Chinese agriculture and forest waste pellets at high heating rates based on the photo-thermal TGA. Energy, 2022, 244, 123164.	4.5	12
6	Behavior Study of Migration and Transformation of Heavy Metals during Oily Sludge Pyrolysis. Energy & Fuels, 2022, 36, 8311-8322.	2.5	16
7	Effects of AAEMs on formation of heavy components in bio-oil during pyrolysis at various temperatures and heating rates. Fuel Processing Technology, 2021, 213, 106690.	3.7	41
8	Simultaneous removal of NO and HgO from flue gas over MnSmCo/Ti catalyst at low temperature. Proceedings of the Combustion Institute, 2021, 38, 5331-5338.	2.4	8
9	Waste tire heat treatment to prepare sulfur self-doped char via pyrolysis and K2FeO4-assisted activation methods. Waste Management, 2021, 125, 145-153.	3.7	12
10	Insights into evolution mechanism of PAHs in coal thermal conversion: A combined experimental and DFT study. Energy, 2021, 222, 119970.	4.5	17
11	Effects of CO2 and H2O on oxy-fuel combustion characteristics and structural evolutions of Zhundong coal pellet at fast heating rate. Fuel, 2021, 294, 120525.	3.4	8
12	An insight into the OPAHs and SPAHs formation mechanisms during alkaline lignin pyrolysis at different temperatures. Journal of Analytical and Applied Pyrolysis, 2021, 156, 105104.	2.6	8
13	Waste Tire Heat Treatment to Prepare Sulfur Self-Doped Char: Operando Insight into Activation Mechanisms Based on the Char Structures Evolution. Processes, 2021, 9, 1622.	1.3	1
14	Experimental and DFT research on role of sodium in NO reduction on char surface under H2O/Ar atmosphere. Fuel, 2021, 302, 121105.	3.4	13
15	Roles of calcium oxide on the evolution of substituted polycyclic aromatic hydrocarbons released from sewage sludge pyrolysis. Journal of Cleaner Production, 2021, 317, 128324.	4.6	14
16	Coke formation and its impacts during electrochemical upgrading of bio-oil. Fuel, 2021, 306, 121664.	3.4	7
17	Steam reforming of typical small organics derived from bio-oil: Correlation of their reaction behaviors with molecular structures. Fuel, 2020, 259, 116214.	3.4	30
18	Chemical imaging of coal in micro-scale with Raman mapping technology. Fuel, 2020, 264, 116826.	3.4	36

#	Article	IF	CITATIONS
19	Effect of temperature on multiple competitive processes for co-production of carbon nanotubes and hydrogen during catalytic reforming of toluene. Fuel, 2020, 264, 116749.	3.4	22
20	Sulfur self-doped char with high specific capacitance derived from waste tire: Effects of pyrolysis temperature. Science of the Total Environment, 2020, 741, 140193.	3.9	43
21	Effects of the Gas-/Liquid-Phase Interactions on the Evolution of Bio-oil during Its Thermal Treatment. Energy & Fuels, 2020, 34, 8482-8492.	2.5	9
22	Evolution characteristics of different types of coke deposition during catalytic removal of biomass tar. Journal of the Energy Institute, 2020, 93, 2497-2504.	2.7	33
23	Pyrolysis of herb waste: Effects of extraction pretreatment on characteristics of bio-oil and biochar. Biomass and Bioenergy, 2020, 143, 105801.	2.9	13
24	A novel integrated pyrolysis-gasification technology for improving quality of bio-gases from multisource solid wastes. IOP Conference Series: Earth and Environmental Science, 2020, 615, 012063.	0.2	0
25	Formation of highly graphitic char derived from phenolic resin carbonization by Ni-Zn-B alloy. Environmental Science and Pollution Research, 2020, 27, 22639-22647.	2.7	11
26	Solidification and Leaching Behaviors of V and As in a Spent Catalyst-Containing Concrete. Energy & Fuels, 2020, 34, 7209-7217.	2.5	5
27	Experimental study and mechanism analysis of NO formation during volatile-N model compounds combustion in H2O/CO2 atmosphere. Fuel, 2020, 273, 117722.	3.4	14
28	Roles of furfural during the thermal treatment of bio-oil at low temperatures. Journal of Energy Chemistry, 2020, 50, 85-95.	7.1	24
29	Evolution of nitrogen/oxygen substituted aromatics from sludge to light and heavy volatiles. Journal of Cleaner Production, 2020, 257, 120327.	4.6	15
30	Efficient Sm modified Mn/TiO2 catalysts for selective catalytic reduction of NO with NH3 at low temperature. Applied Catalysis A: General, 2020, 592, 117413.	2.2	72
31	Promoting effects of Fe-Ni alloy on co-production of H2 and carbon nanotubes during steam reforming of biomass tar over Ni-Fe/α-Al2O3. Fuel, 2020, 276, 118116.	3.4	48
32	Evolution of Aromatic Structures during the Low-Temperature Electrochemical Upgrading of Bio-oil. Energy & Fuels, 2019, 33, 11292-11301.	2.5	154
33	Insights into the highly efficient Co modified MnSm/Ti catalyst for selective catalytic reduction of NO with NH3 at low temperature. Fuel, 2019, 255, 115798.	3.4	38
34	Relationships between structural features and reactivities of coal-chars prepared in CO2 and H2O atmospheres. Fuel, 2019, 258, 116087.	3.4	29
35	Melting solidification and leaching behaviors of V/As during co-combustion of the spent SCR catalyst with coal. Fuel, 2019, 252, 164-171.	3.4	20
36	Effect of La-Modified Supporter on H <sub>2</sub> S Removal Performance of Mn/La/Al <sub>2</sub> O <sub>3</sub> Sorbent in a Reducing Atmosphere. Industrial & Engineering Chemistry Research, 2019, 58, 8260-8270.	1.8	11

#	Article	IF	CITATIONS
37	Formation and reduction of NO from the oxidation of NH3/CH4 with high concentration of H2O. Fuel, 2019, 247, 19-25.	3.4	18
38	Leaching behavior of vanadium from spent SCR catalyst and its immobilization in cement-based solidification/stabilization with sulfurizing agent. Fuel, 2019, 243, 406-412.	3.4	27
39	Effect of the pre-reforming by Fe/bio-char catalyst on a two-stage catalytic steam reforming of bio-oil. Fuel, 2019, 239, 282-289.	3.4	45
40	Formation of the heavy tar during bio-oil pyrolysis: A study based on Fourier transform ion cyclotron resonance mass spectrometry. Fuel, 2019, 239, 108-116.	3.4	42
41	Getting insight into the oxidation of SO2 to SO3 over V2O5-WO3/TiO2 catalysts: Reaction mechanism and effects of NO and NH3. Chemical Engineering Journal, 2019, 361, 1215-1224.	6.6	61
42	Effects of H2O and CO2 on the catalytic oxidation property of V/W/Ti catalysts for SO3 generation. Fuel, 2019, 237, 545-554.	3.4	16
43	The formation mechanism for OPAHs during the cellulose thermal conversion in inert atmosphere at different temperatures based on ESI(â^') FT-ICR MS measurement and density functional theory (DFT). Fuel, 2019, 239, 320-329.	3.4	17
44	Catalytic behaviors of alkali metal salt involved in homogeneous volatile and heterogeneous char reforming in steam gasification of cellulose. Energy Conversion and Management, 2018, 158, 147-155.	4.4	50
45	Evolution of heavy components during sewage sludge pyrolysis: A study using an electrospray ionization Fourier transform ion cyclotron resonance mass spectrometry. Fuel Processing Technology, 2018, 175, 97-103.	3.7	32
46	Hydrogen-Rich Gas Production from Steam Gasification of Lignite Integrated with CO <sub>2</sub> Capture Using Dual Calcium-Based Catalysts: An Experimental and Catalytic Kinetic Study. Energy & Fuels, 2018, 32, 1265-1275.	2.5	7
47	A study of the relationships between coal structures and combustion characteristics: The insights from micro-Raman spectroscopy based on 32 kinds of Chinese coals. Applied Energy, 2018, 212, 46-56.	5.1	102
48	Steam reforming of acetic acid over Ni/Al2O3 catalysts: Correlation of nickel loading with properties and catalytic behaviors of the catalysts. Fuel, 2018, 217, 389-403.	3.4	95
49	Carbon nanotubes formation and its influence on steam reforming of toluene over Ni/Al2O3 catalysts: Roles of catalyst supports. Fuel Processing Technology, 2018, 176, 7-14.	3.7	68
50	Effects of heating rate on the evolution of bio-oil during its pyrolysis. Energy Conversion and Management, 2018, 163, 420-427.	4.4	137
51	Study on the structural evolution of semi-chars and their solvent extracted materials during pyrolysis process of a Chinese low-rank coal. Fuel, 2018, 214, 363-368.	3.4	24
52	Speciation analysis and leaching behaviors of selected trace elements in spent SCR catalyst. Chemosphere, 2018, 207, 440-448.	4.2	45
53	Effects of the component interaction on the formation of aromatic structures during the pyrolysis of bio-oil at various temperatures and heating rates. Fuel, 2018, 233, 461-468.	3.4	37
54	Evolution of coke structures during the pyrolysis of bio-oil at various temperatures and heating rates. Journal of Analytical and Applied Pyrolysis, 2018, 134, 336-342.	2.6	57

#	Article	IF	CITATIONS
55	Pyrolysis of poplar, cellulose and lignin: Effects of acidity and alkalinity of the metal oxide catalysts. Journal of Analytical and Applied Pyrolysis, 2018, 134, 590-605.	2.6	97
56	Relation between char structures and formation of volatiles during the pyrolysis of Shenfu coal: Further understanding on the effects of mobile phase and fixed phase. Fuel Processing Technology, 2018, 178, 379-385.	3.7	19
57	Evolution of structure and activity of char-supported iron catalysts prepared for steam reforming of bio-oil. Fuel Processing Technology, 2017, 158, 180-190.	3.7	41
58	Effects of reaction conditions on the emission behaviors of arsenic, cadmium and lead during sewage sludge pyrolysis. Bioresource Technology, 2017, 236, 138-145.	4.8	68
59	Co-production of hydrogen and carbon nanotubes from the decomposition/reforming of biomass-derived organics over Ni/α-Al2O3 catalyst: Performance of different compounds. Fuel, 2017, 210, 307-314.	3.4	50
60	Mechanistic influences of different solvents on microwave-assisted extraction of Shenfu low-rank coal. Fuel Processing Technology, 2017, 166, 276-281.	3.7	24
61	Molecular structure characterization of the tetrahydrofuran-microwave-extracted portions from three Chinese low-rank coals. Fuel, 2017, 189, 178-185.	3.4	60
62	Thermochemical processing of sewage sludge to energy and fuel: Fundamentals, challenges and considerations. Renewable and Sustainable Energy Reviews, 2017, 80, 888-913.	8.2	428
63	Opposite effects of self-growth amorphous carbon and carbon nanotubes on the reforming of toluene with Ni/α-Al2O3 for hydrogen production. International Journal of Hydrogen Energy, 2017, 42, 14439-14448.	3.8	58
64	Adsorption properties of NO and NH3 over MnOx based catalyst supported on γ-Al2O3. Chemical Engineering Journal, 2016, 302, 570-576.	6.6	57
65	Effects of oxygen species from Fe addition on promoting steam reforming of toluene over Fe–Ni/Al2O3 catalysts. International Journal of Hydrogen Energy, 2016, 41, 17967-17975.	3.8	75
66	Inhibitory effects of CaO/Fe2O3 on arsenic emission during sewage sludge pyrolysis. Bioresource Technology, 2016, 218, 134-139.	4.8	17
67	Performance of CaO for phenol steam reforming and water–gas shift reaction impacted by carbonation process. International Journal of Hydrogen Energy, 2015, 40, 13314-13322.	3.8	15
68	Effects of inherent alkali and alkaline earth metallic species on biomass pyrolysis at different temperatures. Bioresource Technology, 2015, 192, 23-30.	4.8	161
69	Effects of volatile–char interactions on in-situ destruction of nascent tar during the pyrolysis and gasification of biomass. Part II. Roles of steam. Fuel, 2015, 143, 555-562.	3.4	68
70	Catalytic effects of inherent alkali and alkaline earth metallic species on steam gasification of biomass. International Journal of Hydrogen Energy, 2015, 40, 15460-15469.	3.8	162
71	Analysis of mercury species over CuO–MnO2–Fe2O3/γ-Al2O3 catalysts by thermal desorption. Proceedings of the Combustion Institute, 2015, 35, 2847-2853.	2.4	28
72	Ag modified Mn–Ce/γ-Al2O3 catalyst for selective catalytic reduction of NO with NH3 at low-temperature. Fuel Processing Technology, 2015, 135, 66-72.	3.7	96

#	Article	IF	CITATIONS
73	Effects of CO2 and heating rate on the characteristics of chars prepared in CO2 and N2 atmospheres. Fuel, 2015, 142, 243-249.	3.4	65
74	The activity and mechanism study of Fe–Mn–Ce/γ-Al 2 O 3 catalyst for low temperature selective catalytic reduction of NO with NH 3. Fuel, 2015, 139, 232-239.	3.4	177
75	Catalytic oxidation of Hg0 by CuO–MnO2–Fe2O3/γ-Al2O3 catalyst. Chemical Engineering Journal, 2013, 225, 68-75.	6.6	117
76	Influence of different demineralization treatments on physicochemical structure and thermal degradation of biomass. Bioresource Technology, 2013, 146, 254-260.	4.8	179
77	Preparation and characterization of Fe2O3–SiO2 composite and its effect on elemental mercury removal. Chemical Engineering Journal, 2012, 195-196, 218-225.	6.6	86
78	Study on the gas evolution and char structural change during pyrolysis of cotton stalk. Journal of Analytical and Applied Pyrolysis, 2012, 97, 130-136.	2.6	83
79	Influence of cooling rate on structure and combustion reactivity of char during char preparation process. IOP Conference Series: Earth and Environmental Science, 0, 615, 012072.	0.2	0